Numerical Simulation of Combustion with Porous Medium in I.C. Engine

A Mohammadi[1,*] A.Jazayeri[2] M. Ziabasharhagh[3]

[1]PhD Student, [2,3]Associated Professor, Faculty of Mechanical Engineering K.N.TOOSI University of Technology

amohammadi@dena.kntu.ac.ir

Abstract

Porous media has interesting features in compared with free flame combustion due to the extended of the lean flammability limits and lower emissions. Advanced new generation of internal combustion (IC) engines are expected to have far better emissions levels both gaseous and particulate matter, at the same time having far lower fuel consumption on a wide range of operating condition. These criteria could be improved having a homogeneous combustion process in an engine. Present work considers simulation of direct fuel injection in an IC engine equipped with a chemically inert porous medium (PM), having cylindrical geometry that is installed in cylinder head to homogenize and stabilize the combustion process. A numerical study of a 3D model, PM engine is carried out using a modified version of the KIVA-3V code. Since there is not any published material for PM-engines in literature, the numerical results for combustion waves propagation within PM are compared with experimental data available in the literature for a lean mixture of air and methane under filtration in packed bed, the accuracy of results are very promising. For PM-engine simulation the methane fuel is injected directly through a hot PM which is mounted in cylinder head. Therefore volumetric combustion occurs as a result within PM and in-cylinder. The effects of injection timing on mixture formation, pressure and temperature distribution in both phases of PM and in-cylinder fluid together with combustion emissions such as CO and NO are studied in detail for an important part of the cycle.

Keywords: *IC Engine, Porous Medium, Emissions.*

1. INTRODUCTION

The major target for further development of the current IC engines is to reduce their harmful emissions to environment. The most important difficulty with existing IC engines that currently exists is non-homogeneity of mixture formation within the combustion chamber that is the cause of high temperature gradient in combustion chamber which is the main source of excess emissions. At present, the IC engine exhaust gas emission could be reduced by catalyst, but these are costly, with low efficiency. Another strategy has been initiated to avoid the temperature gradient in IC engines that is using homogeneous charge compression ignition (HCCI) engines but there still exist some challenges including, higher unburned hydrocarbon and CO emissions and control of ignition time and rate of heat release under variable engine operating condition [1-3]. Several other technologies have been used to reduce emissions in IC engines, such as electronically controlled high pressure fuel injection systems, variable valve timing, and EGR but these methods still could not solve the problem completely under all engine operating conditions. Thus, whether in IC engines, there is any further potential for development to meet all operational conditions (various load and speed). The demand target may be possible with homogeneous mixture formation and a 3D-ignition of a homogeneous charge to prevent formation of flame front that lead to temperature gradient in the entire combustion chamber. This goal can be achieved by using PM that premixed combustion within PM has been studied together with steady combustion with great success [2, 3]. This technique has been used for both gaseous and liquid fuels in steady or unsteady combustion. Flame stability in PM with lean and rich mixtures and significant reduction in emission with increased

combustion efficiency [4, 5, 6]. Major features of introducing high porosity PM to combustion technology are: having large specific surface area, excellent heat-transfer properties, (high heat capacity) heat capacity, transparency for fluid flow, thermal and mechanical resistance and electrical properties for initiation of combustion [3, 4, 6] (this sentence needs more care). PM-engine is defined as an engine with homogeneous combustion process. The following distinct process of PM-engine is realized in PM volume: energy recirculation in cycle, fuel injection in PM, fuel vaporization for liquid fuels, perfect mixing with air, homogeneity of charge, 3D-thermal self-ignition, and homogeneous combustion. PM-engine may be classified as heat recuperation timing in an engine as: Engine with periodic contact between PM and cylinder is called closed PM-chamber and Engine with permanent contact between PM and cylinder which is called open PM-chamber. (these gigantic sentence need more care) In this paper an open PM-chamber is studied. Permanent contact between working gas and PM-volume is shown schematically in Fig. 1; The PM is placed in engine head. During the intake stroke there is a not much influence from PM-heat capacitor with in-cylinder air thermodynamic conditions. Also during early stages of compression stroke only a small amount of air is in contact with hot PM. The heat transfer process increases during compression, and at TDC the air penetration is cut to the PM volume. At final stages of compression stroke the fuel is injected into PM volume and with liquid fuels rapid fuel vaporization and mixing with air occurs in 3D-structure of PM-volume. Therefore, all essential conditions exist for having homogeneous combustion in the PM engine [7, 8]. The initial idea to use PM in IC engines was proposed by Weclas and Durst in 2001. Their investigation was performed in a single-cylinder air-cooled PM Diesel engine without any catalyst. A silicon carbide (SiC) PM was mounted in the engine head between the intake and exhaust valves and fuel was injected through the PM volume. The implementation has improved engine thermal efficiency, reduced emissions and noise in comparison to the base engine [9, 10].

The effect of SiC PM as a regenerator was simulated by Park and Kaviany in 2002. In their study a PM disk like shape was connected to a rod and was moving near piston within the cylinder of diesel engine. A two-zone thermodynamic model with single-step reaction for methane-air combustion was carried out. It was shown that the maximum cylinder pressure during combustion increases and more work is done during a full cycle, also engine efficiency increases, but due to high temperature of PM that its temperature is higher than adiabatic flame temperature of methane-air, the production of NOx is rather higher, while as its soot decreases [11]. In 2003, Macek and Plasek simulated and studied a PM engine with methane and hydrogen respectively and its potential for practical application was shown [12]. In 2006, Hwan, Ou and Chein mounted a PM on the piston bowl of single-cylinder diesel engine, and observed increase in power and noise reduction relative to original engine due to reduction in maximum pressure. Also, NOx production decreases significantly while, unburned hydrocarbons and soot increase [13]. In 2007 Weclas and Faltermeier investigated penetration of liquid-fuel injection into a PM (as arrangement of cylinders which were mounted on a flat plate with different diameters). The arrangement was changed to obtain optimum geometry which produces the best mixture formation in PM [14]. In 2008, MaoZhao and ZhiGuo studied a PM compression ignition considering an axisymmetric two-dimensional computational domain using KIVA-3V CFD code. In this case the methane was injected directly inside hot PM leading to combustion and the initial temperature of PM and fuel injection time on the mean cylinder temperature and pressure, were studied [15]. In 2008, MaoZhao and ZhiGuo modeled the spray of liquid fuel in an axisymmetrical hot PM with KIVA-3V code, to investigate the effect of injection pressure and spray cone angle in penetration of droplets in PM volume [16]. In 2008, Liu, Wu and Maozaho studied combustion through expansion. The two-zone thermodynamic model was used to investigate the effect of inlet temperature, pressure, compression ratio and excess air on the performance of a PM-engine [17]. In 2009, Liu, Wu and Maozaho investigated the working process of PM engine using an ideal thermodynamic model and predicted the influences of initial temperature on net work done and its efficiency [18].

In this study, 3D-CFD simulation of open PM-engine was carried out with a modified version of KIVA-3V code which methane was injected directly in hot cylindrical PM mounted in the engine head without any optimization for its shapes. Combustion is begun with a very short delay time due to heat supplied by PM. It was demonstrated that PM acts as flame stabilizer. Lack of oxygen existence is clearly visible at the later stages of combustion. Since there were not any published test data available for PM-engines, numerical computations were compared with

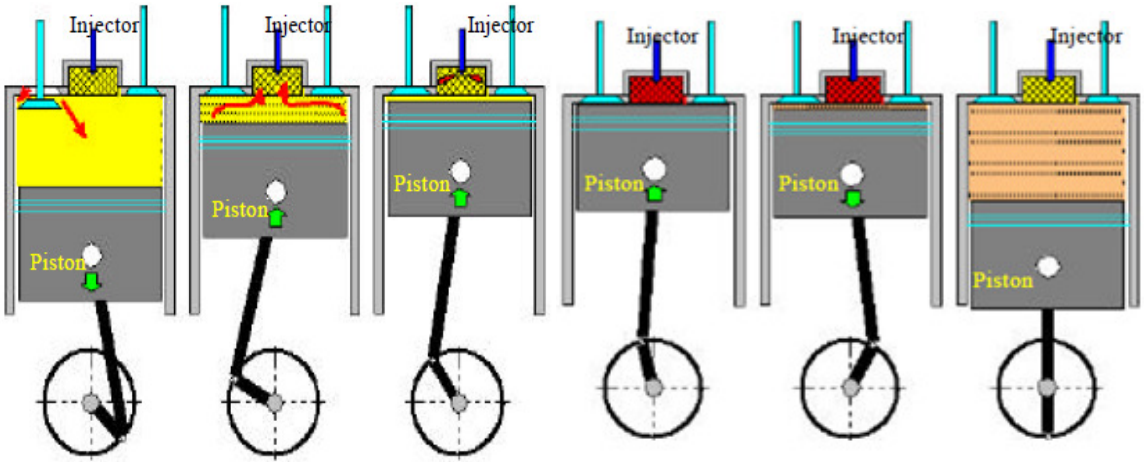

Fig1. A permanent contact PM-engine in operation [10]

experimental data of unsteady combustion wave propagation in a PM by Zhdanok [27]. The accuracy of results could be easily justified by effects of injection time on mean in-cylinder pressure and temperature of solid phase and gas phase in PM, and mass fraction of CH4, CO, NO versus crank angle.

2. Governing Equations

Following assumptions were used in modeling and simulation of the PM:

- There is thermal non-equilibrium between gas and solid phases
- Solid is homogeneous, isotropic, variable property with temperature and has no catalyst effects
-Only radiation heat transfer from the solid phase is considered and the gas phase is transparent

Based on the above assumptions, the general governing equations are simplified as follows [19, 20, 21]:

Continuity equation for species i

$$\frac{\partial(\varphi\rho_i)}{\partial t} + \nabla.(\varphi\rho_i\, u) = \nabla.\left[\rho\ \varphi\ D_{im}\nabla\left(\frac{\rho_i}{\rho}\right)\right] + \varphi\ \dot{\rho}_i^c + \dot{\rho}^s\ \delta_{i1} \quad (1)$$

Where diffusion coefficient modified according to kinetic theory of gases. ρ is mixture density, φ is porosity (void fraction) of porous media, ρi is density of species i, Dim is diffusion coefficient of species i in the mixture and u is the velocity vector.

Gas phase momentum equation

$$\frac{\partial(\rho\, u)}{\partial t} + \nabla.(\rho\, u\, u) = -\frac{1}{a^2}\nabla P - \nabla\left(\frac{2}{3}\,\rho\, k\right) + \nabla.\sigma + F^s - \left(\frac{\Delta P}{\Delta L}\right) \quad (2)$$

The last term on the right-hand side of Eq. (2) is due to pressure drop caused by PM according to Ergan [15] equation and σ is stress tensor. The dimensionless quantity a is used in conjunction with the Pressure Gradient Scaling (PGS) method [20, 21]. This is a method for enhancing computational efficiency in low Mach number flows, where the pressure is nearly uniform.

$$\left(\frac{\Delta P}{\Delta L}\right) = \left(\frac{\mu}{\alpha}\, u + c_2\, \frac{1}{2}\,\rho\,|u|\, u\right) \quad (3)$$

Where α is the permeability and c2 is the inertial resistance factor of PM which both are determined [sentences needs care] according to Eq. 4.

$$\alpha = \frac{d^2}{150}\frac{\epsilon^3}{(1-\epsilon)^2}\ ,\quad c_2 = \frac{3.5}{d}\frac{(1-\epsilon)}{\epsilon^3} \quad (4)$$

Gas phase energy equation

$$\frac{\partial}{\partial t}\left(\varphi\rho c_p T_g\right) + \nabla.\left(\varphi\rho c_p T_g u\right) + \varphi\sum_i \dot{\omega}_i\, h_i W_i = -\varphi P\ \nabla.u + \varphi A_0\rho\epsilon + (1-A_0)\sigma:\nabla u$$
$$\varphi\ \nabla.\left((k_g + \rho_g c_g D_{\parallel}^d)\nabla T_g\right) - h_v\left(T_g - T_s\right) + \dot{Q}^s \quad (5)$$

Where the fourth term on the right hand side is the conduction heat transfer due to thermal conductivity of fluid and dispersion term due to existence of porous media and the fifth term represent the convective heat transfer between gas and solid phase of porous media which are determined according to Eqs. 6, 7, 8:

$$D_{\parallel}^d = 0.5\ \alpha_g\ \mathrm{Pe} \quad (6)$$

$$\mathrm{Nuv}=2+1.1\mathrm{Re}0.6\mathrm{Pr}0.33 \quad (7)$$

$$h_v = \frac{6\varphi}{d^2}\ k_g Nu_v \quad (8)$$

cp is specific heat of the mixture, Tg is gas temperature, Yi is mass fraction species i, ώi is rate of reaction i, hi is enthalpy of species i, Wi is molecular weight of species i, kg is thermal conductivity of the fluid, D‖d is thermal dispersion coefficient along the length of porous media, hv is volumetric heat transfer coefficient between solid and gas phase of porus media. Correlation (6, 7, 8) was estimated from experimental data by Wakao and Kaguei for heat transfer between packed beds and fluid [22].

Solid phase energy equation

$$\frac{\partial}{\partial t}\left((1-\varphi)\,\rho_s\,c_s\,T_s\right) = \nabla\cdot\left[k_s\,(1-\varphi)\nabla T_s\right] + h_v\left(T_g - T_s\right) - \nabla.q_r \quad (9)$$

Ts is solid temperature, ρs is solid density, cs is specific heat of solid phase, ks is thermal conductivity of solid phase, qr is the radiation heat transfer in solid in r direction.

Chemical species conservation equation

$$\frac{\partial}{\partial t}(\varphi\rho Y_i) + \nabla.(\varphi\rho Y_i\,u) + \nabla.(\varphi\rho Y_i\,v_i) - \varphi\,\dot{\omega}_i\,W_i = 0 \quad (10)$$

$$v_i = -\left(D + D^d_{m\|}\right)\frac{1}{X_i}\,\nabla X_i \quad (11)$$

$$Pe = \frac{\rho\,c_{p\,|u|\,d}}{k_g} \quad (12)$$

$$D^d_{m\|} = 0.5\,D_{im}Pe \quad (13)$$

Xi is molar fraction of species i, Pe is Peclet number, d is diameter of sphere in packed bed, Dm‖d is species dispersion coefficient, Yi is mass fraction of species i and vi is diffusion velocity of species i in the mixture.

Turbulence model

Since there is no model presented for simulation of turbulent compressible-flow in PM, by any researcher, hence the basic κ- ε equations were used without any modification. The transport equation for κ turbulent kinetic energy [20]:

$$\frac{\partial(\rho k)}{\partial t} + \nabla.(\rho u\,k) = -\frac{2}{3}\,\rho\,\kappa\,\nabla.u + \sigma:\nabla u + \nabla.\left[\left(\frac{\mu}{Pr_k}\right)\nabla k\right] - \rho\varepsilon + \dot{W}^{\,s} \quad (14)$$

With a similar consideration dissipation rate, ε:

$$\frac{\partial(\rho\varepsilon)}{\partial t} + \nabla.(\rho u\,\varepsilon) - \left(\frac{2}{3}\,c_{\epsilon_1} - c_{\epsilon_3}\right)\rho\,\varepsilon\,\nabla.u + \nabla.\left[\left(\frac{\mu}{Pr_\varepsilon}\right)\nabla\epsilon\right] + \frac{\epsilon}{k}\left[c_{\epsilon_1}\sigma:\nabla u - c_{\epsilon_2}\rho\varepsilon + c_s\,\dot{W}^{\,s}\right] \quad (15)$$

The parameters c_{ϵ_1}, c_{ϵ_2} ,c_{ϵ_3}, Pr_k and $Pr_{\,\varepsilon}$ are constant whose values are determined from experiments and some theoretical considerations and σ is viscous stress tensor [20, 21].

Equation of state

$$P = \rho R\,T_g\,/\,\bar{W} \quad (16)$$

R is universal gas constant, $\bar{W}$ is average molecular weight of mixture; P is pressure inside the combustion chamber.

3. Combustion model

Chemical mechanism for oxidation of methane fuel is considered ώi chemical production rate

$$\dot{\omega}_i = \sum_{i=1}^{NR}\left(v''_{k,i} - v'_{k,i}\right)\,R_i \quad (17)$$

$v''_{k,i}$ and $v'_{k,i}$are stoichiometric coefficients. Combustion process includes ten equations and twelve species. These equations are presented in Table .1, which includes one-step reaction for methane fuel and equations 2-4, are Zeldovich mechanism for NO formation. Rate of reactions [Ri in eq. 17] are computed with Arrhenius method. But for six other equations that reaction rate is very quick relative to last four equations, hence, equilibrium reactions are considered. In order to consider effects of turbulence on combustion the common Eddy-Breakup model [21, 23] has been used.

Table1. Kinetic and equilibrium reactions

Number	Equation
1	$CH4 + 2\,O_2 \rightarrow CO_2 + 2\,H_2O$
2	$O2 + 2\,N2 \rightarrow 2\,N + 2\,NO$
3	$2\,O2 + N2 \rightarrow 2\,O + 2\,NO$
4	$N2 + 2\,OH \rightarrow 2\,H + 2\,NO$
5	$H_2 \leftrightarrows 2\,H$
6	$O_2 \leftrightarrows 2\,O$
7	$N_2 \leftrightarrows 2N$
8	$O + H \leftrightarrows O\,H$
9	$O_2 + 2\,H_2O \leftrightarrows 4\,OH$
10	$O_2 + 2\,CO \leftrightarrows 2\,CO_2$

The combustion model used is Spalding's eddy-break up model [23, 24]. Spalding suggested that combustion processes are best described by focusing attention on coherent bodies of gas, which squeezed and stretched during their travel through the flame. This model relates the local and instantaneous turbulent combustion rate to the fuel mass fraction and the characteristic time scale of turbulence. The application of this model requires adjustment of a specific coefficient and ignition time to match the experimental combustion rate with the computational combustion rate. In this case, the Coefficients of model were determined from experimental analysis of conventional engine [24].

4. Radiation model

Due to extreme temperature of combustion zone and solid phase, radiation heat transfer is very important. Gas phase radiation in comparison with solid phase radiation that has a high absorption coefficient is negligible. Several relations for modeling of radiation heat transfer and derived radiation intensity are presented. The heat source term $\nabla . q_r$, due to radiation in solid phase that appears in Eq .9, can be calculated from Roseland model [25].

$$q_r = -\frac{16}{3}\frac{\sigma {T_s}^3}{\beta}\nabla T_s \qquad (18)$$

Where σ is Boltzmann constant and β is extinction coefficient.

5. Gas injection model

Methane in gas form is directly injected downward from the top center of a disk-like shape hot PM volume. The new gas injection model is used [26], for simulating transient direct injection of gaseous phase fuel into combustion chamber through a practical computational grid.

Mesh Preparation

Engine specifications and PM data have been presented in Table. 2. Prior to CFD simulation, computational mesh of engine was generated with Kiva-Prep. The geometry of a mesh is composed of two numbers of logical blocks (PM and in-cylinder) that are patched together in a seamless fashion. Patching allows geometry to be created, block by block. Fig. 2 shows the grid configuration of the engine at top dead center (TDC). Mesh size ranged from about 238144 at BDC (7744 grid in PM and 223744 grid in-cylinder) to about 22144 at TDC (7744 in PM and 14400 in-cylinder) for computational studies. Computational domain is composed of two-cylinders, top cylinder is PM space and bottom is in-cylinder volume. Grid variation and maximum pressure in a closed cycle are presented In Table. 3. The solutions highlights mesh independency since with increasing grids from 21144 to 22686 at TDC, no variation in the pressure profile is observed.

chamber, since there is no data published about wall temperature of PM-engine.

Table2. Engine and PM specifications

Displacement volume	0.981 liter
Bore	102 mm
Stroke	120 mm
Nominal compression ratio (without PM)	18
Connecting rod length	192 mm
Engine speed	2000 rpm
Mass of injected methane	0.0055 g
Equivalence ratio	0.17
Height of PM	15 mm
Diameter of PM	30 mm
porosity	0.8

6. Initial and Boundary Conditions

Computation starts at bottom dead center (BDC). Initial charge densities were calculated based on temperature of 300 K for fluid flow, and 1200 K for solid phase of PM at BDC. The standard κ-ε turbulence model in the code was used with an initial value of turbulent kinetic energy κ, assumed 10 percent of the total kinetic energy based on the mean piston speed that assumed to be uniform. Radial velocity is initialized assuming a swirl ratio 0. The entire wall boundary was assumed as zero heat-flux for fluid and also solid phase of PM and combustion

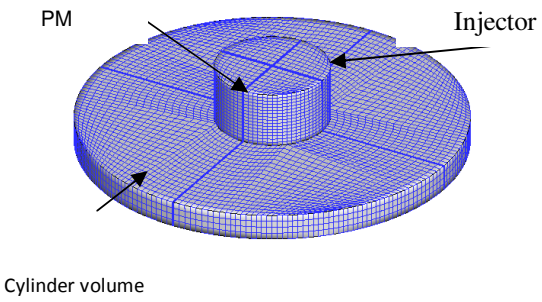

Fig2.. Computational mesh for CFD calculation at TDC

Table 3. Maximum pressure variations of with mesh size

Mesh size at top dead center	Maximum pressure in cycle	Crank angle at maximum pressure
18756	4723452	359
19176	4807655	360
21144	4996756	360
22628	4996769	360

7. Computational Procedures

The KIVA-3V is an open source code that can deal with transient three dimensional chemically reactive flows with sprays, was used to solve the in cylinder flow and solid phase calculations. Species, momentum, energy, and turbulence transports equations are solved using finite volume method, which subdivides fluid domain of computation into a number of hexahedron cells. Solutions are marched in a number of cycles or time steps, in which the transports [transport is true] equations are solved in three phases namely, phase A, B, and C. Phase A calculates spray droplet collision and oscillation terms and source term due to spray and chemistry while diffusion, viscous, and pressure gradient terms are solved in a coupled and implicit fashion in phase B. The solution procedure is very similar to the SIMPLE scheme, and each individual equation is solved iteratively using conjugate residual method [19, 20, 21]. In Phase C, the flow field is remapped onto a new computational mesh, which is essentially calculating the convective transport terms. In the case of non moving mesh problem, the mesh is mapped back onto its original location (Phase B calculation where fluid mesh moving with the flow); in the case of moving boundary problem, the mesh is mapped to a new location. Phase C is calculated in a sub cycled and fully explicit fashion.

8. Validation

For validate purposes of numerical simulations, a modified KIVA-3V code for simulation of unsteady combustion is a cylindrical porous-tube together with experiments data available by Zhdanok et al. was used [27-29]. The test section is a vertical quartz glass tube with 1300 mm in length and 76 mm in diameter, which is isolated from the environment. The test section was filled with a packed bed of 5.6 mm solid-alumina spheres. For simulation a cylinder with 76 mm in diameter and 600 mm in length that filled with PM, was considered. The boundary condition applied to the momentum and energy equations with the assumption of zero gradients for both phase of PM and species transport through the downstream boundary. At the upstream boundary, the gas temperature is 300K, composition is premixed methane-air with equivalence ratio 0.15, velocity is 0.43 m/s for the premixed reactants and zero gradient for solid phase, were specified. For initial temperature for both phase of PM experimental measured data was used. Fuel is methane, porosity of PM is 0.4 [27] and flow assumed laminar for this simulation. Fig. 3 plots a comparison of simulation results to the experimental results of Zhdanok et al. at the time of 147 s. The calculated speed of combustion waves are in very good agreement with experimental results. From Fig. 3, methane is completely consumed in flame front through combustion wave propagation and in this location maximum temperature is noticeable.

9. Results and Discussion

Figs. 4a, 4b show that mass fraction of methane in a chamber without PM respectively, after 10 and 20 degree crank angle, where the start of injection was 30 degree crank angle before TDC (the parentheses are unnecessary) . Injector is installed in cylinder head and is align and parallel to the cylinder axis and injects fuel straight downward direction. Typical installation has been chosen without any preferences for optimization (Fig. 2). Injected fuel temperature is set to be 300 K and initial temperature of two phase of PM in BDC (the parentheses are unnecessary) is the same as temperature injected fuel. Cold injection with no combustion has considered without having PM in place.

Diffusion of gas in chamber is absolutely visible by studying Figs. 4a, 4b. After 10 degree crank angle of injection, methane impinges on piston surface and disperses in the cylinder volume. Figs. 5a, 5b, show mass fraction of methane as the same conditions as Figs. 4a, 4b, except that the effect of PM was spotted. It is clear that after 10 and 20 degree of injection, methane completely placed in PM space and disperses in it, but very rich air-fuel mixture is seen near the injector in PM space and this could be a problem that it needs attention during combustion process.

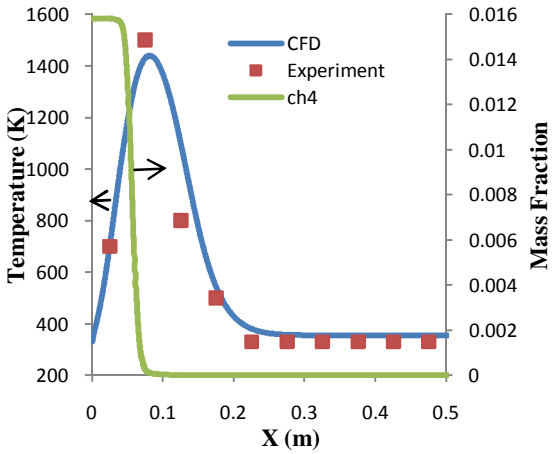

Fig3.. Comparison of combustion wave propagation between CFD calculation and experiment data for time 147s

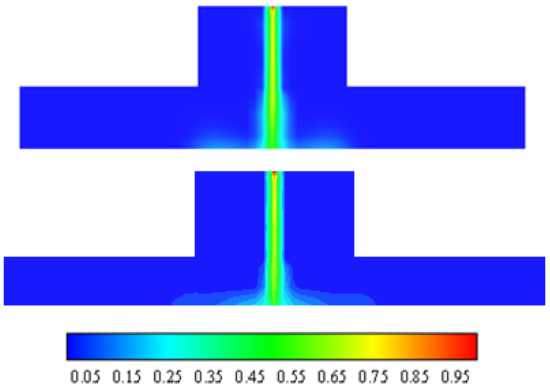

Fig4. Mass fraction of methane at location x=0 for cold injection timing of 10 and 20 degrees angle without having PM in place respectively.

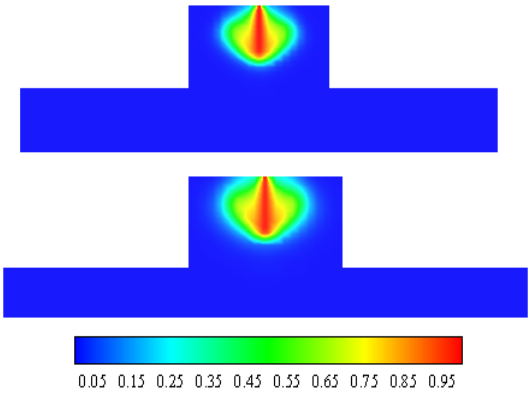

Fig5. Mass fraction of methane at location x=0 for cold injection timing 10 and 20 degrees angle without with having PM in place respectively

Diffusion of gas in chamber is absolutely visible by studying Figs. 4a, 4b. After 10 degree crank angle of injection, methane impinges on piston surface and disperses in the cylinder volume. Figs. 5a, 5b, show mass fraction of methane as the same conditions as Figs. 4a, 4b, except that the effect of PM was spotted. It is clear that after 10 and 20 degree of injection, methane completely placed in PM space and disperses

in it, but very rich air-fuel mixture is seen near the injector in PM space and this could be a problem that it needs attention during combustion process.

Comparison between Figs. 4, 5 highlights the effect of PM on dispersion of fuel and mixture formation. PM can disperse the methane in its volume and prohibits diffusion of methane to in-cylinder space. This is a great advantage for lean mixture, because most part of combustion could take place in PM volume and part of heat release absorbs with solid phase of PM. Hence, bulk-fluid temperature decreases and has a major effect on NO reduction relative to conventional combustion. Also, new features for PM could be explored if inclined angle relative to engine axis is selected for injection or several holes for injector rather than only one hole for injector which is considered in this case so better dispersion of methane in PM space can take place. For both case of having PM in place or not having it, the mass fraction of methane is between 0.05 to 0.95, but having PM would give a far better dispersion of fuel.

Figs. 6 to 11 show the distribution of methane, oxygen, carbon dioxide, carbon monoxide, temperature in fluid and solid phase in PM and in-cylinder as results of combustion, for several different crank angle 325, 360, and 415. Start of injection is 300 degree crank angle and duration of injection for 60 degree crank angle, to decrease injection pressure of methane and more time for better mixture formation, in this case the fuel injection duration is not optimized. In Fig. 6 mass fraction of methane for different crank angle, with having combustion in PM-engine, from 325 to 415 degree crank angle.

Also from Fig. 6 it can be concluded that due to timing, localized fuel injection and combustion unburned fuel resulted from blow-by does not exist.

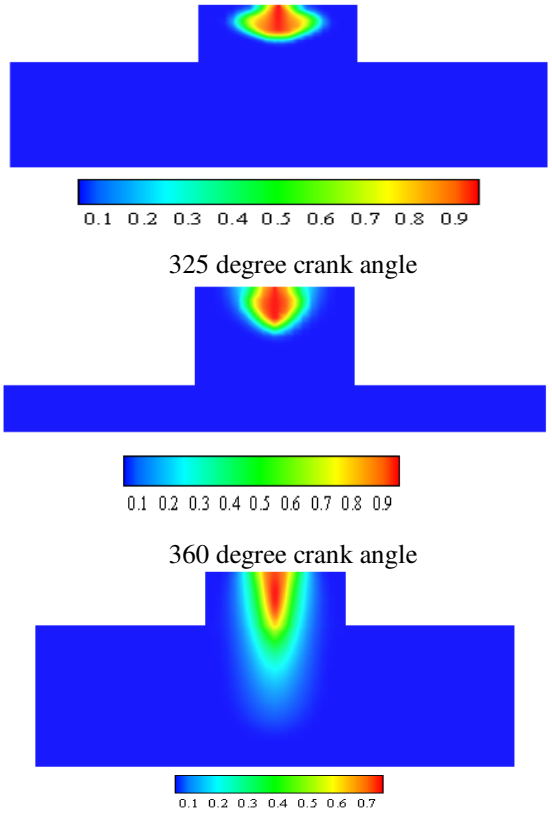

Fig6. Mass fraction of methane at location x=0 with having combustion for different crank angle

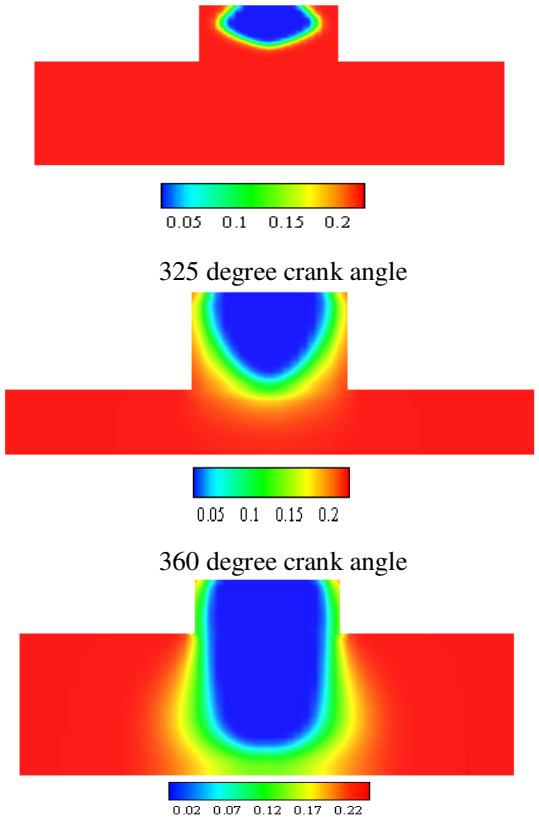

Fig7. Mass fraction of oxygen at location x=0 with having combustion for different crank angle

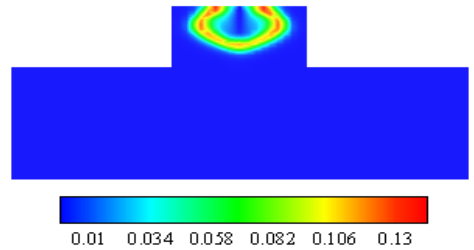

325 degree crank angle

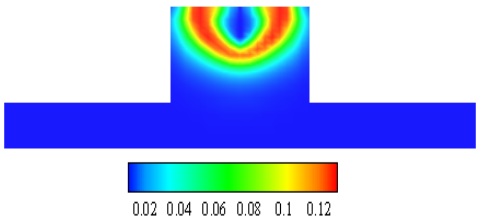

360 degree crank angle

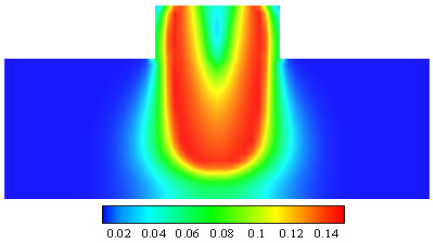

415 degree crank angle

Fig8. Mass fraction of carbon-dioxide at location x=0 for different crank angle

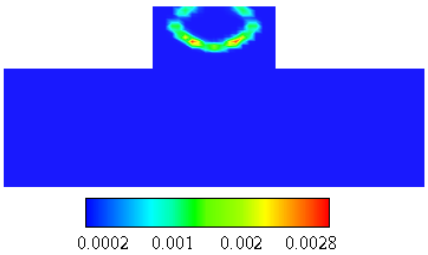

325 degree crank angle

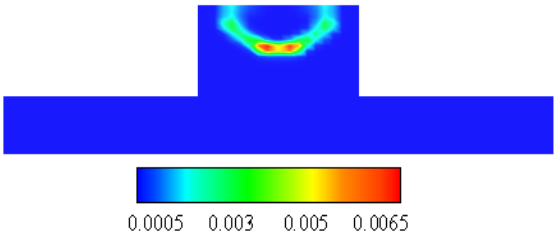

360 degree crank angle

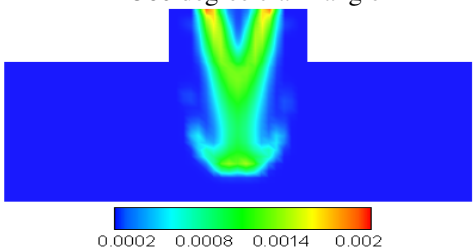

415 degree crank angle

Fig9.. Mass fraction of carbon-monoxide at location x=0 for different crank angle

In Fig .7 mass fraction of oxygen for different crank angle from 325 to 415 degree crank angle, during combustion process is shown. It can be seen that oxygen near the injector consumes rapidly and thereby residual methane in PM does not access to enough oxygen at last stage of combustion, therefore some methane residues are left over in PM

Fig. 8 shows mass fraction of carbon dioxide for different crank angle during combustion process from 325 to 415 degree crank angle. It is shown that reactions occur in the flame front in PM that is a wide region relative to normal flame front in conventional engines and carbon dioxide forms in a region between injector and flame front.

In Fig. 9 mass fraction of CO for different crank angle during combustion process from 325 to 415 degree crank angle, is shown. Carbon monoxide is formed around flame front near thy in-cylinder space. Maximum mass fraction of CO is about 0.0065 in TDC.

In Fig .10 temperature distribution of fluid in different crank angle from 325 to 415 degree crank angle is shown. Flame front is recognizable from high temperature region in PM. Maximum fluid temperature in TDC is about 2200 K, but this is a local value of maximum temperature and mean average temperature is much lower than this value is about 1500 K. Also, due to existence of solid phase in PM, some heat release of combustion is absorbed by

This phase and so prevents from high temperature gradient in fluid. Fig. 11 shows temperature distribution in solid phase of PM from 325 to 415 degree crank angle. Temperature near the injector is

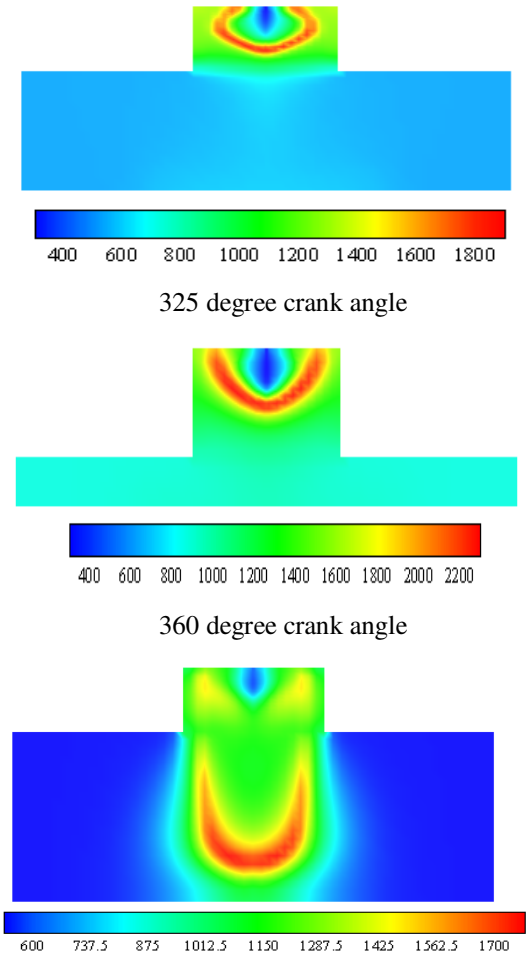

Fig10. Temperature distribution of fluid in at location x=0 with combustion for different crank angle

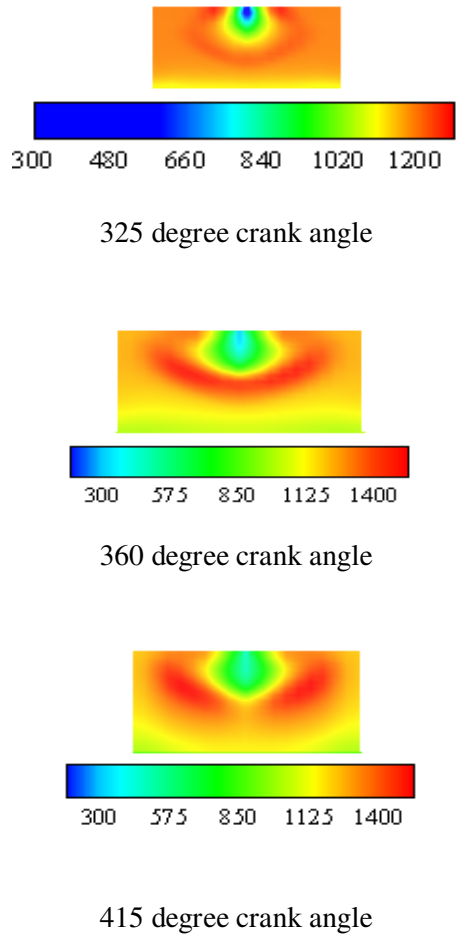

Fig11. Temperature distribution in solid phase of PM in at location x=0 with combustion for different crank angle

about 300 K because fuel injected in hot PM with this temperature, then fuel absorbs heat of solid phase of PM near the injector and temperature of methane raises in a short distance from injector and reaches to self-igniting temperature and combustion occurs instantly with not much delay although solid phase of PM has high heat capacity with low temperature variation in it.

10. Effect of injection time

Figs. 12 and 13 show numerical results for mean pressure and temperature distribution in combustion chamber versus crank angle. Simulation was started from BDC (180 degree crank angle). During engine motoring, no fuel is injected inside PM and only heat exchange is between in-cylinder air and solid phase of PM. The maximum pressure in motoring condition is about 45.5 bar that occurs at TDC. For five different injection timing (300, 310, 320, 330, 340 crank angle degree) with 10 degree duration for injection, the mean cylinder pressure versus crank angle, during of combustion are considered.

It is shown that pressure distribution does not depend on injection time and maximum pressure is about 50 bar for all five cases. From Fig. 13 maximum temperature (bulk temperature of all fluid in PM and in-cylinder flow) in motoring condition is about 920 K and all investigation is carried out. For five injection time (same time as Fig. 12), the mean cylinder temperature versus crank angle are seen. It is shown that the maximum temperature does not depend on injection time and maximum temperature is about 940 K for all five cases. It should be noticed that with this very low equivalence ratio ($\Phi = 0.17$),

combustion cannot be started in conventional engine but with porous media technology, it is possible to use very lean mixture for in-cylinder combustion.

Figs. 14 and 15 show the results for distribution of temperature in both phase of PM (solid and fluid) for five different crank angle injection times (300-340 degree). Simulation is started at BDC, initial fluid and solid phase temperatures respectively were 300 K and 1200 K but optimal temperature for PM solid phase for best performance of engine, was not determined yet. It is noted that temperature in both phases of PM, does not change significantly with the variation of the injection time. Maximum value of temperature in PM is about 1480 K in gas phase and 1280 K in solid phase. As expected in the combustion process, gas temperature is higher than the solid temperature and heat is absorbs with solid phase due to high heat capacity of it. It is seen that injection time after 330 degree crank angle (like 340 degree) lead to reduction of mean temperature in both phases of PM than earlier injection timing, because lower amount of methane consumes and so lower heat release occurs.

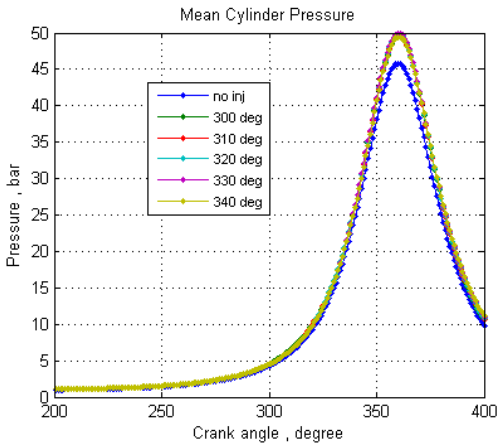

Fig12. Mean pressure distribution in cylinder versus crank angle

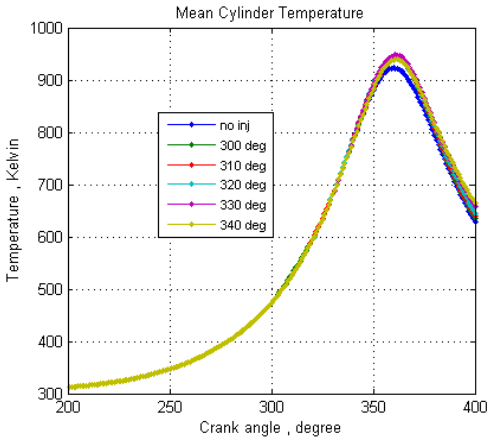

Fig13. Fluid mean temperature distribution in cylinder versus crank angle

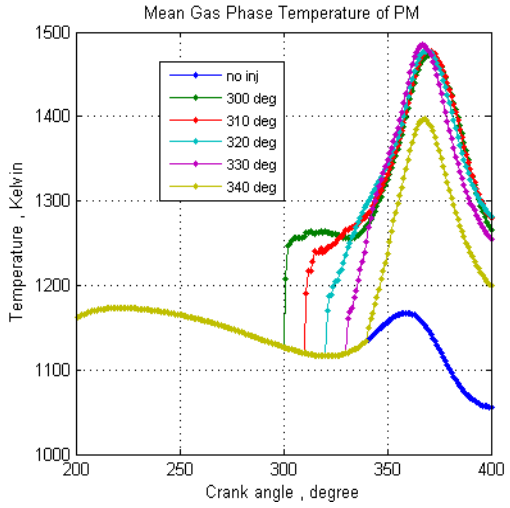

Fig14. . Mean temperature distribution in gas phase of PM versus crank angle

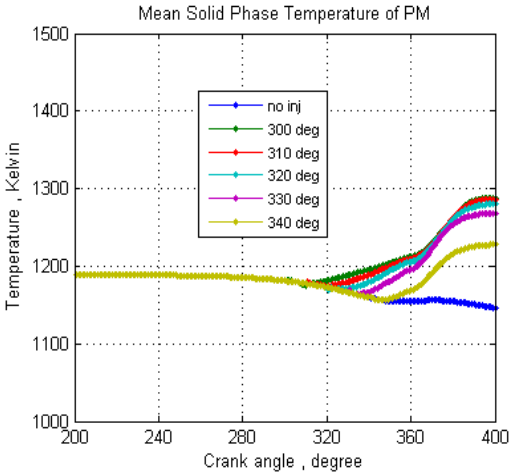

Fig15. . Mean temperature distribution in solid phase of PM versus crank angle

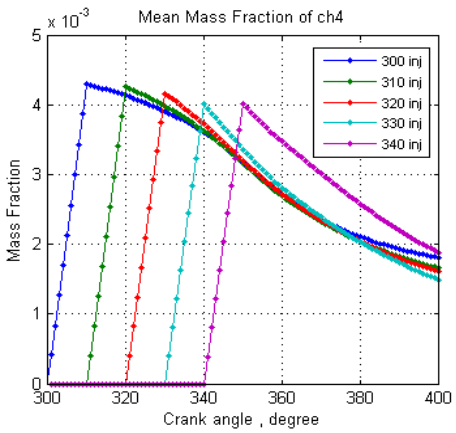

Fig16. . Mass fraction of methane versus crank angle

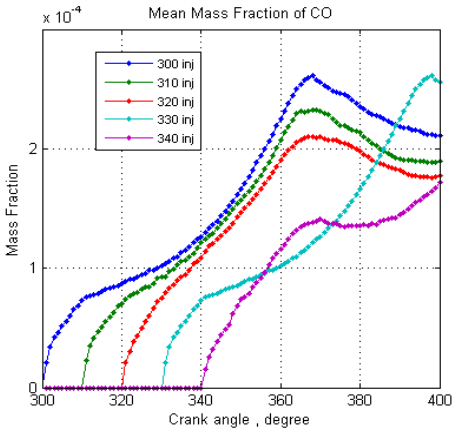

Fig17. . Mass fraction of CO versus crank angle

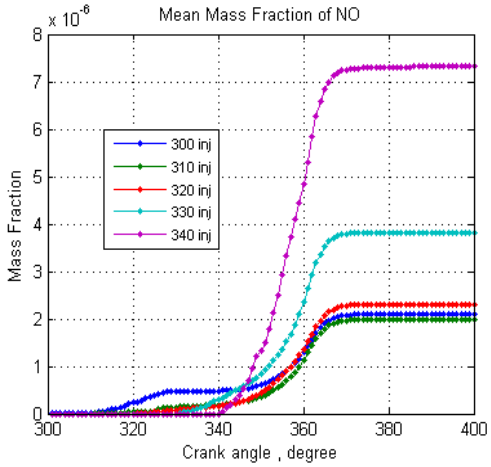

Fig18. Figure 18. Mass fraction of NO versus crank angle

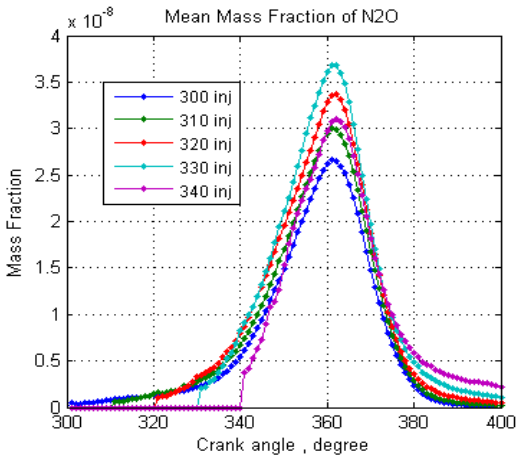

Fig19. Figure 19. Mass fraction of N_2O versus crank angle

Fig. 16 shows mean mass fraction of methane in combustion chamber for five different injection times (300-340 degree).Results indicates that, some of the fuel is consumed very rapidly after the injection time but due to lack of accessibility of oxygen in near flame front some of the injected methane residues in cylinder which correspond to Figs. 6, 7. In form of unburned hydrocarbon which stays in the cylinder which this has to be resolved by some means.

Figs. 17 and 18 show mass fraction of CO and NO versus crank angle. Carbon monoxide is formed right at the beginning of fuel injection and almost instantaneous and combustion of methane-air mixture later after 10 degree increases gradually and its concentration reaches to maximum value in

366 degree crank angle and then decreases with completion of combustion where CO is converted to CO2. From Fig. 17 due to unsteady nature of combustion in PM some of CO molecules have not enough time to react with O2 molecules and convert to CO2 molecules. It is concluded that later injection time after 320 degree crank angle increases production of CO than early injection time (300, 310, 320 degree), but still its value is very lower than conventional engines but in any case it is far better to avoid late injection.

Fig. 18 indicates that the amount of NO before injection time is negligible due to low in-cylinder temperature. Later with the start of combustion, PM temperature increases as shown in Fig. 14.

Drastic reduction in temperature lowers the production of NO to almost nothing. But due to the fact that the fluid temperature about 1500 K is considerably lower than normal combustion in common engines, production of NO is very lower relative to production of NO in normal operating

condition of IC engines. Approximately after 370 degree crank angle. There is no further change in No value and its mass fraction is about $2\times10^{-6.}$

Again like the CO production, late injection of methane (later than 320 degree) causes to increase in NO value to two or three times of early injection time (300, 310 and 320 degree). So, although late injection has not considerable effect on mean cylinder pressure, but late injection results in further change in NO value.

In Fig. 19 mass fraction of N2O versus crank angle, for five different injection time is shown and it is indicated that variation of injection time from 300 to 330 degree lead to increasing the amount of N2O, but its mass fraction is about 2×10^{-8} and is very lower relative to mass fraction of NO that is about 2×10^{-6}. So, in this type of engine production of N2O is not considerable.

11. Conclusions

Application of a cylindrical PM in an IC engine using methane injection in a hot PM was modeled and simulated through modified version of KIVA-3V code. A detail study of contours for mass fraction of methane, oxygen, carbon dioxide, carbon monoxide and temperature in both phase of PM was carried out. The effects of injection timing on in-cylinder mean pressure, temperature also emissions concentration of CO and NO versus crank angle, was investigated. Following results are obtained:

1) Combustion using a very lean air-fuel ratio (Φ = 0.17), is possible by application of porous media technology, in an IC engine, while it would be out of question in a conventional engine.

2) A perfect cylindrical geometries with sharp angle and corner are not appropriate choice for PM engine since air cannot penetrates to PM interior easily and mixes with methane fuel but there is possibility of using air- assist injector to enhance air accessibility for better combustion of methane within PM.

3) Start of injection does not have a major effect on in-cylinder pressure and temperature but late injection increases the production of CO and NO.

4) In expansion stroke still some unburned methane remains in combustion chamber due to lack of accessibility of oxygen in time.

5) At early stage of expansion for almost any injection duration solid phase of PM prevents the temperature of gas phase and combustion products to increase so this reduces the NO production drastically.

References

[1]. Stanglmaier, R. H., Roberts, C. E., "Homogeneous charge compression ignition: benefits, compromises and future engine applications", SAE Paper 1999-01-3682, 1999.

[2]. Weclas, M., "Potential of porous medium combustion technology as applied to internal combustion engine", MECA/AECC Meeting, Nurnberg, Germany, 2001.

[3]. Durst, F., Weclas, M., "Strategy for intelligent internal combustion engine with homogeneous combustion in cylinder", MECA/AECC Meeting, Nurnberg, Germany, 2003.

[4]. Trim, D., Durst, F., "Combustion in porous medium – advances and application", J. Combustion Science and Technology, Vol. 121, pp. 153-168, 1996.

[5]. Kamal, A. A., Mohammad, A. A., "Combustion in porous media", Proc. IMeche, Vol. 220, pp. 478-509, 2006.

[6]. Mujeebu, A. A., Abdullah, M. Z., Mohammad, A. A., Bakar, M. Z. A., "Trend in modeling of porous media combustion", J. Progress in Energy and Combustion Science, Vol. 2, pp. 1-24, 2010.

[7]. Weclas, M., " Strategy for intelligent internal combustion engine with homogeneous combustion in cylinder", Sonderdruck Schriftenreihe University of Applied Sciences in Nuernberg, No. 26, pp. 1–14, 2004.

[8]. Weclas, M., Porous media in internal combustion engine, Scheffle, M. P., Colombo, editors, Cellular ceramics-structure , manufacturing, properties and application, Wiley, 2005.

[9]. Durst, F., Weclas, M, "A new type of internal combustion engine based on the porous medium technology", J. Proc Inst Mech. Eng, Vol. 215, pp. 63-81, 2001.

[10]. Durst, F., Weclas, M., "A new concept of I.C. engine with homogeneous combustion in a porous medium", The Fifth International Symposium on Diagnostic and Modeling of Combustion in Internal Combustion Engines, Nagoya, Japan, 2001.

[11]. Park, C. W., Kaviany, M., "Evaporating combustion affected by in cylinder reciprocating porous regenerator", ASME J. Heat Transfer, Vol. 124, pp. 184-194, 2002.

[12]. Polasek, M., Macek, J., "Homogenization of combustion in cylinder of CI engine using porous medium", SAE Paper 2003-01-1085, 2003.
[13]. Le, D. C., Chein, C. J., Kwak, Y. H., "Improving surface characteristic of porous media reactor in diesel engine by plasma technology", F2006C27 conference, 2006.
[14]. Weclas, M., Faltermeier, R., "Diesel jet impingement on small cylindrical obstacles for mixture homogenization by late injection strategy", Int. J. Engine Research, Vol. 8, pp. 399-413, 2007.
[15]. Zhigou, Z., Mahozhao, X., "Numerical study on the compression ignition of a porous medium engine", Springer, Vol. 51, No. 3, pp. 277-287, 2008.
[16]. Zhigou, Z., Mahozhao, X., "Numerical simulation about interaction between pressure swirl spray and hot porous medium", J. Energy Conversion & Management, Vol. 49, pp. 1047-1055, 2008.
[17]. Hongsheng, L., Maozaho, X., Shi, C., Hong, L., "Simulation of porous media engine using a two-zone combustion model", SAE Paper 2008-01-1516, 2008.
[18]. Hongsheng, L., Maozaho, X., Shi, C., Hong, L., "Regenerative cycle in porous medium engine", J. Energy Conversion and Management, Vol. 59, pp. 273-303, 2009.
[19]. Mohammadi, A., Numerical simulation of spark Ignition engines, Numerical simulations – Examples and Applications in Computational Fluid Dynamics, Lutz Angermann (Ed.), ISBN: 978-953-307-153-4, InTech, Austria, 2010.
[20]. [20] Amsden, A. A., O'Rourke, P. J., and Butler, T. D., " KIVA-II: A computer program for chemically reactive flows with sprays", Los Alamos National Laboratory Report LA-11560-MS, Los Alamos, 1989.
[21]. Amsden, A. A., "KIVA-3V: A block-structured KIVA program for engines with vertical or canted valves", Los Alamos National Laboratory Report LA-13313-MS, Los Alamos, 1997.
[22]. Wakao, N., and Kaguei, S., Heat and mass transfer in packed beds, Gordon and Breach Science Publications, New York, USA, 1982.
[23]. Magnussen, B. F., and Hjertager, B. H., "On mathematical modeling of turbulent combustion with special emphasis on soot formation and combustion", The Sixteenth Int. Symp. on Combustion,The Combustion Institute, Pittsburgh, 1977.
[24]. Turn, S. R., An introduction to combustion, McGraw-Hill, New York, pp. 399-400, 1996.
[25]. Modest, M. F., Radiative heat transfer, Academic Press, California, USA, 2003.
[26]. Ra, Y., Kong, S. C., Reitz, R. D., Rutland, C. J., Han, Z., "Multi dimensional modeling of transient gas jet injection using coarse computational grids", SAE Paper 2005-01-0208, 2005.
[27]. [Zhdanok, S.,"Super adiabatic combustion of methane air mixture under filtration in a packed bed", J. Combustion and Flame, Vol. 100, pp. 221-231, 1995.
[28]. Henneke, M. R., Jellzey, J. L., "Modeling of filtration combustion in a packed bed", J. Combustion and Flame, Vol. 117, pp. 832-840, 1999.
[29]. Bubmivich, V. I., Zhdanok, S. A., Dobrego, K. V., "Analytical study of methane-air mixture in a packed bed", Int. J. Heat and Mass Transfer, Vol. 49, pp. 2578-2586, 2006